# ATP SYNTHESIS AND DEGRADATION RATES IN THE PERFUSED RAT HEART

## $^{31}$P–Nuclear Magnetic Resonance Double Saturation Transfer Measurements

RICHARD G. S. SPENCER,* JAMES A. BALSCHI,* JOHN S. LEIGH, JR.,‡
AND JOANNE S. INGWALL*
*NMR Laboratory, Harvard Medical School, Boston, Massachusetts 02115; and ‡Departments of Biochemistry and Biophysics, and Radiology, University of Pennsylvania, Philadelphia, Pennsylvania 19104

ABSTRACT A limitation of magnetization transfer techniques for studying enzyme kinetics in vivo has been the difficulty of treating systems with more than two exchanging species. This problem was addressed in the original papers describing saturation transfer. Since then, a number of approaches have been devised to study these complex situations. Here, we present a method based on the transient saturation transfer experiment in which spin-lattice relaxation time constants and reaction rates are obtained from the same magnetization transfer data. This technique is particularly suitable for biological samples. We apply the method to evaluate flux balance in the three-site linear exchange network composed of ATP, creatine phosphate, and inorganic phosphate in the isolated, perfused rat heart and show that the method yields reasonable values for the reaction velocities of ATP synthesis and degradation.

### INTRODUCTION

Saturation transfer methods provide kinetic information characterizing two-site exchange when applied to a system in which there are only two reactants, or in which reactions between all but two species may be neglected. In addition, one can obtain the spin-lattice relaxation times, $T_1$, of both species. Biological and other complex chemical systems are frequently characterized by the presence of multiple, competing reactions. In these cases, application of standard single-resonance saturation transfer techniques yields results that are valid only in certain limiting cases. Moreover, approaches that neglect the presence of competing reactions can lead to apparent violations of the principle of detailed balance. For example, Nunnally and Hollis (1), Matthews et al. (2), Kobayashi et al. (3), and Bittl and Ingwall (4) all performed saturation transfer experiments of the intact beating heart at moderate to high levels of cardiac performance in which either the ([$\gamma$-P]ATP) or creatine phosphate (CP) resonance was saturated. Unidirectional fluxes through the creatine kinase reaction, CP $\rightleftharpoons$ ATP, were calculated. This reaction scheme will be referred to as the two-site model for phosphorus exchange. All four investigations (1–4) reported that the flux towards ATP synthesis was greater than the flux towards CP synthesis. Furthermore, this discrepancy increased as cardiac work increased. This result is inconsistent with the fact that ATP and CP concentrations in the well-oxygenated perfused heart are constant at a given level of cardiac work. Because CP participates only in the creatine kinase reaction, saturation transfer should provide a reliable measure of CP degradation. However, ATP is known to participate in many other reactions; furthermore, fluxes through these ATP-utilizing reactions depend on the physiological state of the heart (e.g., increased ATP utilization due to higher contractile demands). Thus, the presence of these competing reactions invalidates straightforward saturation transfer measurements of flux from ATP to CP. To a degree depending upon the relative flux of ATP through competing reactions, the value obtained for the forward creatine kinase reaction flux by saturating CP differs from the value obtained for the reverse reaction, obtained by saturating ([$\gamma$-P]ATP).

Thus, an extension of usual single-resonance saturation transfer methods is required to account for the presence of competing reactions. This problem was recognized by Forsen and Hoffman (5), who presented a direct extension of their original theory (6, 7) of transient saturation transfer to the N-site system, allowing for simultaneous exchange between each pair of sites. Since then, other work

Dr. Balschi's current address is Division of Cardiovascular Disease, University of Alabama at Birmingham, Cardiovascular NMR Laboratory, CMRL Building, University Station, Birmingham, Alabama 35294.

Address correspondence to Joanne S. Ingwall, Ph.D., Harvard Medical School, NMR Laboratory, 221 Longwood Avenue, Room 209, Boston, MA 02115.

(8) on the multisite exchange problem has centered on steady-state saturation techniques in which spin-lattice relaxation times are determined in one set of experiments, and then used along with the results of a separate experiment to derive kinetic constants. Both the transient method of Forsen and Hoffman and these steady-state methods extend the single-resonance saturation technique by saturating two resonances simultaneously. Ugurbil (9, 10), adapting the steady-state approach, was the first to apply a multiple saturation technique to an in vivo system, namely, the creatine kinase reaction, in the perfused rat heart.

In the work described here, we study this same enzymatic system, i.e., the phosphorus exchange network in the heart, using a variation of the original Forsen and Hoffman transient saturation transfer method, which has two important advantages over steady-state methods for in vivo studies. First, in our transient experiments, the reaction rates and spin-lattice relaxation times are derived from the same data set rather than from data produced from independent experiments. This ensures that both quantities reflect the same state of the sample. This is a nontrivial issue, given the inherent instability of most biological samples and the long times needed to perform a saturation-transfer experiment. Second, as discussed by Koretsky and Weiner (11), the $T_1$'s obtained by the two methods would differ if one of the reactants is composed of two NMR-visible pools, one of which is exchanging and the other which is not exchanging. In this case, as we will show, steady-state methods cannot provide information about the chemical–kinetic lifetimes or abundances of the two compartments, or about the reaction rate itself. On the other hand, transient methods such as those used in the present study could be used in conjunction with inversion–recovery experiments to determine the lifetimes and abundances of the two pools and also to permit the exchange rate to be defined without confounding contributions from the presence of the nonexchanging pool.

## METHODS

### Theory

We will modify the two-site exchange network

$$\mathrm{A} \underset{k_{BA}}{\overset{k_{AB}}{\rightleftharpoons}} \mathrm{B} \tag{1}$$

by the addition of a third reactant, C, defining the following simple system of competing reactions:

$$\mathrm{A} \underset{k_{BA}}{\overset{k_{AB}}{\rightleftharpoons}} \mathrm{B} \underset{k_{CB}}{\overset{k_{BC}}{\rightleftharpoons}} \mathrm{C}, \tag{2}$$

where $k_{AB}$, $k_{BA}$, $k_{BC}$, and $k_{CB}$ denote pseudo–first-order rate constants. In the model of cardiac energetics that we will later be concerned with, we will take species A = CP, B = ATP, and C = $P_i$, so that the reaction between A and B is the creatine kinase reaction, and the reaction between B and C represents the sum of all ATPase reactions. The equations of motion for the magnetizations are

$$\frac{dM(A)}{dt} = \frac{M_0(A) - M(A)}{T_1(A)} - k_{AB}M(A) + k_{BA}M(B) \tag{3}$$

$$\frac{dM(B)}{dt} = \frac{M_0(B) - M(B)}{T_1(B)} - (k_{BA} + k_{BC})M(B) + k_{AB}M(A) + k_{CB}M(C) \tag{4}$$

$$\frac{dM(C)}{dt} = \frac{M_0(C) - M(C)}{T_1(C)} - k_{CB}M(C) + k_{BC}M(B), \tag{5}$$

where $T_1(S)$ denotes the longitudinal relaxation time, $M_0(S)$ is the equilibrium magnetization, and $M(S)$ is the instantaneous value of the magnetization, for species S.

First, a conventional single-resonance saturation transfer experiment may be performed on this system in which the magnetization of species B is nulled. During the time in which $M(B) = 0$, the evolutions of $M(A)$ and $M(C)$ are governed by

$$\frac{dM(A)}{dt} = \frac{M_0(A)}{T_1(A)} - \frac{M(A)}{\tau(A)} \tag{6}$$

$$\frac{dM(C)}{dt} = \frac{M_0(C)}{T_1(C)} - \frac{M(C)}{\tau(C)}, \tag{7}$$

where $1/\tau(A) = 1/T_1(A) + k_{AB}$, and $1/\tau(C) = 1/T_1(C) + k_{CB}$. Eqs. 6 and 7 have the solution

$$\frac{M(S)(t)}{M_0(S)} = 1 - k_{SB}\tau(S)\left\{1 - \exp\left[\frac{-t}{\tau(S)}\right]\right\}, \tag{8}$$

where the species label S = A or C.

Obtaining measurements for a sequence of saturation times $t$ yields a curve of $M(S)(t)/M_0(S)$ vs. $t$. This curve is parameterized by the constants $k_{SB}$ and $T_1(S)$, which can therefore be determined by a two-parameter fit of the data to Eq. 8. Defining the chemical flux from species S to species R by $F_{SR} = k_{SR}M_0(S)$, we see that from the $k_{SB}$'s and measurements of $M_0(S)$ in the absence of saturation, we may obtain the magnetization fluxes $F_{AB} = k_{AB}M_0(A)$ from A to B and $F_{CB} = k_{CB}M_0(C)$ from C to B.

If we now invoke the steady-state chemical conditions $F_{BA} = F_{AB}$, $F_{BC} = F_{CB}$, we need go no further in investigating the fluxes out of B into A and C. Using detailed balance, the remaining rate constants may be derived from the two already obtained. However, this ignores the possibility that the reaction scheme as written is incomplete. To test this, we require a direct measurement of the total flux out of B, $F_{BA} + F_{BC} = (k_{BA} + k_{BC})M_0(B)$, for comparison with the total flux into B, $F_{AB} + F_{CB}$.

If the results of a single saturation at A of the network Eq. 2 were used to estimate either $k_{BA}$ or $(k_{BA} + k_{BC})$, the result would be an underestimate of these quantities, and hence of $F_{BA}$ or of $(F_{BA} + F_{BC})$. This is most easily seen by considering a steady-state saturation-transfer experiment.

For the three-site exchange network (Eq. 2), a long-time

saturation of A yields the pair of algebraic equations

$$0 = \frac{M_0(B) - M(B)}{T_1(B)} - (k_{BA} + k_{BC})M(B) + k_{AB}M(A) + k_{CB}M(C) \quad (9)$$

$$0 = \frac{M_0(C) - M(C)}{T_1(C)} - k_{CB}M(C) + k_{BC}M(B). \quad (10)$$

Solving simultaneously for the steady-state measured value of $M(B)$, [that is, $M_{ss}(B)$], one finds readily

$$\frac{M_{SS}(B)}{M_0(B)} = \frac{1 + k_{BC}T_1(B) + k_{CB}T_1(C)}{1 + (k_{BA} + k_{BC})T_1(B) + k_{CB}T_1(C) + k_{BA}k_{CB}T_1(B)T_1(C)}. \quad (11)$$

On the other hand, suppose that one assumes that the exchange network Eq. 1 is valid. The derived reaction rate, $k'_{BA}$, which may be regarded as an estimate of $k_{BA}$ or of $k_{BA} + k_{BC}$, satisfies

$$\frac{M_{SS}(B)}{M_0(B)} = \frac{1}{1 + T_1(B)k'_{BA}}. \quad (12)$$

Upon solving Eqs. 11 and 12 for the estimate $k'_{BA}$ in terms of the true $k_{BA}$, we find

$$k'_{BA} = k_{BA}\left[1 - \frac{k_{BC}T_1(B)}{1 + k_{CB}T_1(C) + k_{BC}T_1(B)}\right]. \quad (13)$$

Note that this $k'_{BA}$ satisfies $k'_{BA} < k_{BA} < k_{BA} + k_{BC}$. Thus, assuming the validity of Eq. 1 results in an underestimate of the flux out of B by an amount dependent upon the relative magnitudes of $k_{BC}T_1(B)$ and $k_{CB}T_1(C)$.

Thus, the discrepancy between the forward and reverse fluxes through the creatine kinase reaction found in references 1–4 could result from a truncation of the phosphorus exchange network Eq. 2 to the simpler network Eq. 1. A measurement of these fluxes at high cardiac workload which properly accounts for the three-site network Eq. 2 is required to test this hypothesis.

This can be done in the following fashion. Consider the three-site model, Eqs. 2–5. By simultaneously saturating sites A and C for a time $t$, we obtain, for the evolution of $M(B)$ during the saturation,

$$\frac{dM(B)}{dt} = \frac{M_0(B)}{T_1(B)} - \left[k_{BA} + k_{BC} + \frac{1}{T_1(B)}\right]M_0(B). \quad (14)$$

The solution to this equation is identical in form to that of Eqs. 6 and 7, and is

$$\frac{M(B)(t)}{M_0(B)} = \left(1 - (k_{BA} + k_{BC})\tau(B)\left\{1 - \exp\left[\frac{-t}{\tau(B)}\right]\right\}\right), \quad (15)$$

where $1/\tau(B) = 1/T_1(B) + (k_{BA} + k_{BC})$. A two-parameter fit of double-saturation data to Eq. 15 now gives $(k_{BA} + k_{BC})$ and $T_1(B)$. From the former, we can calculate the total magnetization flux out of B, $F_{BA} + F_{BC} = (k_{BA} + k_{BC})M_0(B)$.

If the three-site exchange network shown in Eq. 2 is adequate to describe NMR-observable fluxes between species A, B, and C, we expect that the sum of $F_{AB}$ (derived from fitting data to the solution of Eq. 6) and $F_{CB}$ (derived from fitting data to the solution of Eq. 7) will be equal to $(F_{BA} + F_{BC})$ (derived from fitting data to Eq. 15):

$$F_{AB} + F_{CB} = F_{BA} + F_{BC}. \quad (16)$$

We have applied this approach to study the chemical fluxes maintaining constant ATP concentration in the perfused rat heart, to determine whether the simplest three-site model for phosphorus exchange

$$CP \underset{k_r}{\overset{k_f}{\rightleftharpoons}} ATP \underset{k'_f}{\overset{k'_r}{\rightleftharpoons}} P_i, \quad (17)$$

where f forward and r reverse, with the associated Bloch equations

$$\frac{dM(CP)}{dt} = \frac{M_0(CP) - M(CP)}{T_1(CP)} - k_fM(CP) + k_rM([\gamma\text{-P}]ATP) \quad (18)$$

$$\frac{dM([\gamma\text{-P}]ATP)}{dT} = \frac{M_0([\gamma\text{-P}]ATP) - M([\gamma\text{-P}]ATP)}{T_1([\gamma\text{-P}]ATP)} - (k_r + k'_r)M([\gamma\text{-P}]ATP) + k_fM(CP) + k'_fM(P_i) \quad (19)$$

$$\frac{dM(P_i)}{dt} = \frac{M_0(P_i) - M(P_i)}{T_1(P_i)} - k'_fM(P_i) + k'_rM([\gamma\text{-P}]ATP) \quad (20)$$

is adequate to describe NMR-observable fluxes of phosphorus in this system.

## Isolated Perfused Rat Heart

For each experiment, a male Sprague-Dawley rat weighing 350–400 g was anesthetized with an intraperitoneal injection of 40 mg sodium pentobarbital. The heart was rapidly excised and immersed in ice-cold buffer. The aorta was then dissected free, and the heart was attached to a perfusion apparatus as described previously (12). The heart was perfused retrograde through the aorta with phosphate-free Krebs-Henseleit buffer gassed with 95% $O_2$ and 5% $CO_2$ (pH 7.4). The buffer was composed of (mM) NaCl (118), KCl (4.7), EDTA (0.5), $MgSO_4$ (1.2), $CaCl_2$ (1.75), $NaHCO_3$ (25), and glucose (11). Temperature was maintained at 37°C. A constant-pressure system was used, providing a perfusion pressure of 100 mmHg under gravity feed.

## Hemodynamic Measurements

A water-filled latex balloon was inserted into the left ventricle through an incision into the left atrium, via the

mitral valve. By adjusting the volume of this balloon, preload, and hence the product of heart rate and developed pressure (systolic minus diastolic pressure), i.e., the rate-pressure product (RPP), could be adjusted in all hearts. Left-ventricular systolic and diastolic pressures were measured via a water-filled tube running from the balloon to a Statham P23Db pressure transducer, connected to a Hewlett-Packard physiological recorder. Systolic and diastolic pressures were monitored continously throughout the experiment. By adjusting preload, we achieved two different workloads, with RPP of 22,000 and 32,000 mmHg/min, respectively. Hearts were excluded if their rate–pressure products could not be closely adjusted to one of these two values.

### $^{31}$P-NMR Measurements

The perfused hearts were placed into a 20-mm sample tube and inserted into the bore of an Oxford Instruments 360 wide-bore magnet (field strength, 8.46 Tesla) interfaced with a Nicolet 1280 computer.

$^{31}$P-NMR spectra were obtained at 145.75 MHz with 60° broadband observation pulses, with a minimum interpulse delay of 3 s. Each spectrum was the Fourier transform of the average of 76 free-induction decays, with an applied line broadening of 20 Hz. Low-power saturations were applied either at [$\gamma$-P]ATP or at $P_i$ and CP for 0, 0.3, 0.6, 1.2, 2.4, and 4.8 s for each set of kinetic data acquisition. Loss of intensity due to saturation transfer for each time-point was assessed by measurement of peak heights (after fitting the spectral lines to a Lorentzian form).

The power input to the sample is a major determinant of the value of the equilibrium magnetization of a saturated resonance, and, to a lesser extent, the time required to achieve this equilibrium saturation. In these experiments, the power delivered to the sample from the saturating beam was of the order of 0.5 W. It could be adjusted continuously over a wide range through the use of a variable series resistance. For perfused rat heart experiments with the NMR probe used in the present work, the time required to achieve saturation with this power is ~10 ms, which is only 3% of the shortest duration of saturation used.

The degree to which a resonance was saturated in these experiments was defined by the residual magnetization along the axis of the main magnetic field. This residual magnetization was assessed by measuring the observed magnetization of the resonance following a nonselective observation pulse. By use of the variable resistance, we were able to achieve essentially complete saturation of desired resonances with minimal saturation of adjacent resonances.

Spillover to the adjacent CP peak during single saturation at ([$\gamma$-P]ATP) was measured by moving the saturating frequency upfield of CP by an amount equal to the frequency separation between ([$\gamma$-P]ATP) and CP. Measured in this way, direct spillover saturation of CP during ([$\gamma$-P]ATP) saturation was <10%.

For the simultaneous saturation at $P_i$ and CP, we mixed the output of an audio frequency oscillator with a low-power narrowband radio frequency carrier signal from the spectrometer. The carrier signal was placed halfway between the $P_i$ and CP resonances, and the audio frequency mixed was equal to one-half of the spacing between these peaks. Direct spillover saturation of ([$\gamma$-P]ATP) during simultaneous saturation at $P_i$ and CP was estimated by placing the carrier upfield of [$\beta$-P]ATP by an amount equal to the upfield distance of the carrier from ([$\gamma$-P]ATP) during double saturation. Assessed in this way, spillover during the double resonance saturation experiments, averaged from baseline saturations of seven hearts, was <10%.

Hearts were excluded from the study if they showed metabolic instability (defined as ≥10% change in NMR-measured metabolite levels) or hemodynamic instability (defined as ≥10% change in RPP) during the course of an experiment. Both single ([$\gamma$-P]ATP) and double ($P_i$ and CP) resonance saturation measurements were obtained on each heart.

### Data Analysis

In accordance with Eqs. 8 and 15, the results of each transient saturation transfer protocol, composed of the full sequence of saturation times, were fitted to the form

$$f(t; a, b) = \left\{1 - a \cdot b \cdot \left[1 - \exp\left(\frac{-t}{b}\right)\right]\right\},$$

by the nonlinear least-squares routine of the RS/1 software of BBN Research Systems, Cambridge, Massachusetts. The best-fit values of $a$ and $b$ give, respectively, $k$ and $\tau$ for each of the two saturation protocols on each heart. $T_1$ was then derived from these values. The $T_1$'s and $k$'s so obtained were then averaged; errors are given as the standard error of the mean (SEM) of this average.

Fluxes were derived by multiplying the $k$'s and the relative metabolite levels obtained by integrating the $P_i$, [$\beta$-P]ATP, and CP resonances of each heart, with the integral of [$\beta$-P]ATP arbitrarily set to 100 magnetization units. In each heart, the metabolite levels were measured at the beginning and end of each of the two saturation transfer protocols to confirm metabolic stability.

All errors are presented as ± SEM. Errors in derived quantities (e.g., fluxes and ratios) were calculated using propagation of errors, assuming that the errors in the factors are independent (13).

## RESULTS

Fig. 1 shows stacks of NMR spectra obtained from single and double resonance saturation experiments of the same heart. For single resonance saturation transfer (Fig. 1 *A*), transfer of saturation from ([$\gamma$-P]ATP) to $P_i$ and to CP is

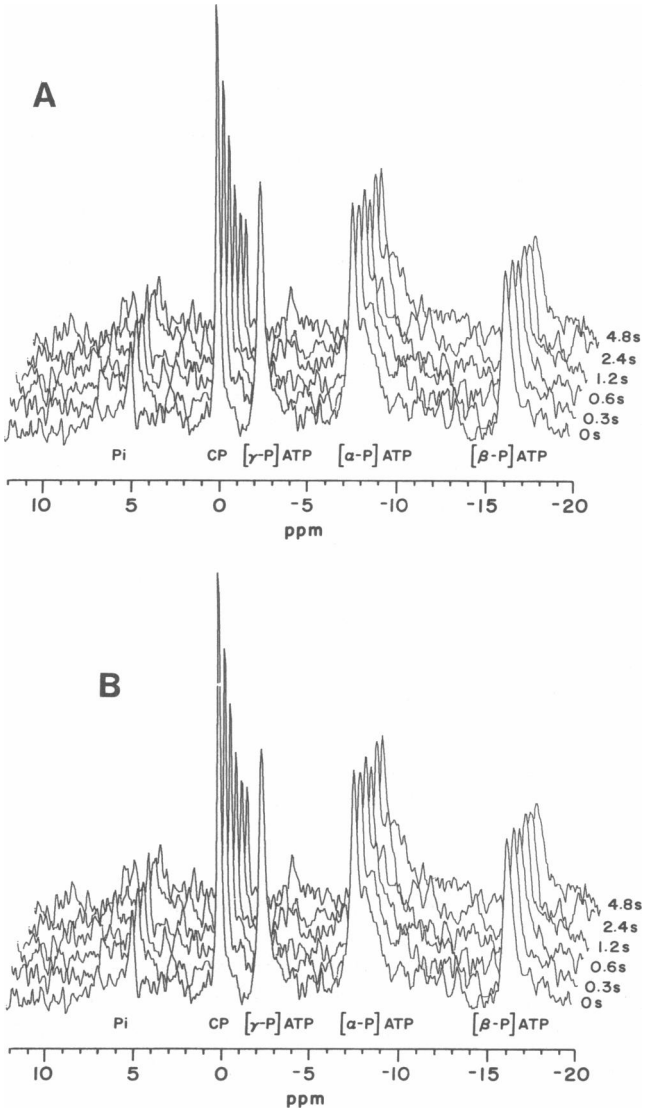


FIGURE 1 $^{31}$P-NMR spectra from the two saturation protocols performed on isolated buffer-perfused rat hearts. Time of saturation is indicated to the right of each spectrum. (*A*) Transient saturation of [γ-P]ATP, allowing measurement of $T_1(P_i)$, $T_1(CP)$, $k'_f$, and $k_f$. (*B*) Simultaneous transient saturation of $P_i$ and CP, allowing measurement of $T_1([\gamma\text{-P}]ATP)$, and $(k_r + k'_r)$.

shown by the gradual decline of their magnetizations as the saturation time increases. Fitting the data to monoexponential functions, we derived values for $k_f$, $k'_f$, $T_1(P_i)$, and $T_1(CP)$ (Table I). At a rate–pressure product of 22,000 mmHg/min, the total signal losses in the $P_i$ and CP peaks after a 4.8-s saturation of ([γ-P]ATP) were 35 and 71%, respectively (averaged over all experiments). After 4.8 s of saturation, the observed magnetization loss due to saturation transfer has reached nearly a steady state, so that the residual peak intensities should also satisfy relationships analogous to Eq. 12:

$$\frac{M_{ss}(P_i)}{M_0(P_i)} = \frac{1}{[1 + k'_f \cdot T_1(P_i)]} \tag{21}$$

and

$$\frac{M_{ss}(CP)}{M_0(CP)} = \frac{1}{[1 + k_f \cdot T_1(CP)]}. \tag{22}$$

Using the derived values of $k'_f$, $k_f$, $T_1(P_i)$, and $T_1(CP)$, it is seen that these equations are approximately satisfied. Of course, exact equality is not to be expected, since in the present technique, $T_1$'s and $k$'s are derived from the entire transient saturation transfer data set, rather than from equilibrium values alone. Similar results are obtained from the experiments performed at the higher rate–pressure product.

Fig. 1 *B* shows spectra obtained from simultaneous saturation of $P_i$ and CP. Transfer of saturation to ([γ-P]ATP) is shown by the monoexponential decline of its magnetization as a function of saturation time, from which $(k_r + k'_r)$ and $T_1([\gamma\text{-P}]ATP)$ are obtained. At a rate–pressure product of 22,000 mmHg/min, the total signal loss in the ([γ-P]ATP) peak after a 4.8-s saturation of $P_i$ and CP was 39% (averaged over all experiments). In this case, we expect the relationship

$$\frac{M_{ss}([\gamma\text{-P}]ATP)}{M_0([\gamma\text{-P}]ATP)} = \frac{1}{[1 + (k_r + k'_r) \cdot T_1([\gamma\text{-P}]ATP)]} \tag{23}$$

to be approximately satisfied. Using the values of $(k_r + k'_r)$ and $T_1([\gamma\text{-P}]ATP)$ derived from the entire data set, it is seen that this is indeed the case. Again, similar results are obtained at 32,000 mmHg/min.

In each heart, the pseudo first-order rate constants $k_f$, $k'_f$, and $(k_r + k'_r)$, defined by the proposed three-site exchange network shown in Eq. 17 and the Bloch Eqs. 18–20, were obtained by using the two transient saturation transfer network shown in Eq. 17 and the Bloch Eqs. 18–20, were obtained by using the two transient saturation transfer protocols. These were combined with equilibrium magnetizations obtained from spectra without saturation to derive the fluxes $F_f = k_f[CP]$, $F'_f = k'_f[P_i]$, and $F_r + F'_r = k_r[ATP] + k'_r[ATP]$. With these quantities, we can assess the adequacy of Eq. 17 to account for ATP homeostasis in the heart. This is done by checking whether the total phosphorus flux of ATP synthesis equals the total flux of ATP degradation, $F_f + F'_f = F_r + F'_r$, as required by detailed balance.

A complete set of experiments was performed at each of two workloads, defined respectively by RPP = 22,000 mmHg/min and RPP = 32,000 mmHg/min. The lower workload was selected to match the one workload reported previously (4) that showed a statistically significant difference between $F_f$ and $F_r$. The higher workload provided an additional check on the method, since, as a result of higher energy demands and hence greater activity of ATPase systems, the discrepancy between $F_f$ and $F_r$ measured by standard single-peak saturation transfer would be expected to be even greater.

The quantities measured in the NMR experiments at each workload were: the relative concentrations of CP,

TABLE I
MEASURED AND DERIVED NMR AND KINETIC PARAMETERS

| | RPP = 22,000 mmHg/min, $n$ = 5 | | | RPP = 32,000 mmHg/min, $n$ = 5 | | |
|---|---|---|---|---|---|---|
| | Measured quantities | | | Measured quantities | | |
| | CP | [γ-P]ATP | $P_i$ | CP | [γ-P]ATP | $P_i$ |
| $M_0$ | 109 ± 3.8 | 100 ± 3.5 | 28 ± 1.3 | 110 ± 5.4 | 100 ± 4.7 | 34.3 ± 2.4 |
| $T_1$ | 2.78 ± 0.16 | 0.64 ± 0.13 | 2.4 ± 0.31 | 3.00 ± 0.46 | 0.82 ± 0.12 | 1.92 ± 0.22 |
| | $k_f$ | $k_r + k'_r$ | $k'_f$ | $k_f$ | $k_r + k'_r$ | $k'_f$ |
| | 0.90 ± 0.08 | 1.15 ± 0.19 | 0.37 ± 0.09 | 0.92 ± 0.06 | 1.04 ± 0.13 | 0.63 ± 0.22 |
| | Derived quantities | | | Derived quantities | | |
| | $F_f$ | $k_r$ | | $F_f$ | $k_r$ | |
| | 98.1 ± 9.4 | 0.98 ± 0.1 | | 101 ± 8.7 | 1.02 ± 0.1 | |
| | $F'_f$ | $k'_r$ | | $F'_f$ | $k'_r$ | |
| | 10.4 ± 2.6 | 0.10 ± 0.03 | | 21.6 ± 5.0 | 0.22 ± 0.05 | |
| | $F_{syn}$ | $F_{deg}$ | | $F_{syn}$ | $F_{deg}$ | |
| | 108 ± 9.3 | 115 ± 19.0 | | 123 ± 10.0 | 104 ± 13.7 | |
| | $F_{syn}/F_{deg}$ | $F_{CK}/F_{ATPase}$ | | $F_{syn}/F_{deg}$ | $F_{CK}/F_{ATPase}$ | |
| | 0.94 ± 0.18 | 9.4 ± 2.5 | | 1.18 ± 0.18 | 4.68 ± 1.16 | |

NMR-derived reaction rates and spin-lattice relaxation times are shown for all metabolites at both workloads. Magnetizations are in arbitrary units. For the purpose of calculating fluxes, the mean of $M_0$([γ-P]ATP) has been set to 100. The SEM is derived from the SEM of the ratio of $M_0$([γ-P]ATP) to $M_0$ ([γ-P]ATP) to $M_0$ ([β-P]ATP). $k$'s have the units of 1/s, $T_1$'s are in seconds, and fluxes are in magnetization units per second. Fluxes are derived as described in the text. Results for the lower rate–pressure product of 22,000 mmHg/min are shown in the first column, while results for the higher rate–pressure product of 32,000 mmHg/min are shown in the second column. The derived $k_r$ and $k'_r$ are obtained from detailed balance, and so are not used in the calculation of $F_{deg}$. Instead, $F_{deg}$ is derived from the measured sum $(k_r + k'_r)$.

([γ-P]ATP), and $P_i$; the spin-lattice relaxation times $T_1$(CP), $T_1$([γ-P]ATP), and $T_1(P_i)$; and the kinetic constants $k_f$, $(k_r + k'_r)$, and $k'_f$. Of these, the double resonance saturation technique is required to obtain correct values only for $T_1$([γ-P]ATP) and $(k_r + k'_r)$, while standard single resonance saturation-transfer experiments suffice to obtain $T_1$(CP), $T_1(P_i)$, $k_f$, and $k'_f$.

From the experimental data, we derived:

$F_{CK}$ = flux through the creatine kinase reaction

$= k_f$[CP],

$F_{ATPase}$ = flux through ATPases = $k'_f[P_i]$,

$F_{syn}$ = total ATP synthesis = $k_f$[CP] + $k'_f[P_i]$, and

$F_{deg}$ = total ATP degradation = $(k_r + k'_r)$[[γ − P]ATP].

The values of the measured quantities and the fluxes are given in Table I. There were no significant differences in any of the measured or derived quantities between the two workloads investigated.

The primary result of this study is that the three-site model, Eq. 17, is indeed adequate to demonstrate detailed balance in the combined creatine kinase–ATPase system of the heart and to demonstrate ATP homeostasis. As shown in Table I and Fig. 2, the ratio of the phosphorus flux of ATP synthesis to the flux of ATP degradation at each of the two workloads was indistinguishable from unity: at RPP = 22,000 mmHg/min, $F_{syn}/F_{deg}$ = 0.94 ± 0.18, while at RPP = 32,000 mmHg/min, $F_{syn}/F_{deg}$ = 1.18 ± 0.18.

Fig. 2 also shows a direct comparison between the present study and results presented reference 4, in which the reverse creatine kinase reaction was analyzed with saturation applied only at CP. As shown above, single-

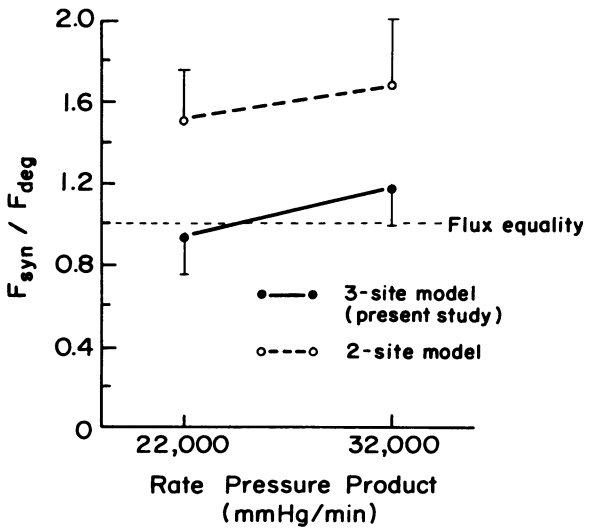


FIGURE 2 Ratio of the flux towards ATP synthesis, $F_{syn}$, to the flux towards ATP degradation, $F_{deg}$, derived at rate–pressure products of 22,000 and 32,000 in the present study and in reference 4. In reference 4, this ratio differed from unity, whereas in the present study it did not.

saturation would be expected to underestimate the rate of ATP degradation. In fact, as seen in Fig. 2, at a workload of 22,000 mmHg/min, the single-saturation experiment underestimated $F_{deg}$; the apparent $F_{syn}/F_{deg} = 1.51 \pm 0.25$. In contrast, the double-saturation treatment of $F_{deg}$ lowers this ratio to $0.94 \pm 0.18$, a value indistinguishable from unity. At a higher workload of 32,000 mmHg/min, the discrepancy between synthesis and degradation flux using single resonance saturation is still greater, $F_{syn}/F_{deg} = 1.69 \pm 0.33$, whereas, using the method described in the present study, this ratio is $F_{syn}/F_{deg} = 1.18 \pm 0.18$, again indistinguishable from the expected value of unity.

The data shown in Table I can also be used to calculate the P:O ratio for ATP synthesis by oxidative phosphorylation. By using a literature value for ATP concentration of 22 μmol/g dry wt, we calculate a unidirectional ATP synthesis rate from NMR measurements of 2.3 and 4.8 μmol g dry $wt^{-1}s^{-1}$ for workloads of 22,000 and 32,000 mmHg/min, respectively. Using literature values of 0.84 and 1.12 μmol g dry $wt^{-1}s^{-1}$ for oxygen consumption (4), we calculate P:O ratios of 2.7 and 4.2 for these two workloads. Within the errors of the measurements, these values are indistinguishable. The large errors result principally from errors in the derived reaction rates, resonance areas, and measurements of oxygen consumption.

## DISCUSSION

The reaction kinetics of a chemically exchanging system in steady-state is constrained by the appropriate statement of the law of detailed balance. Given this, a saturation transfer experiment can be used to test the validity of an assumed reaction network.

To take the simplest example, consider again the two-site network, Eq. 1. Saturation transfer experiments may be performed to determine $k_{AB}$, and, separately, $k_{BA}$. If the reaction network as written is correct, then

$$k_{AB} = k_{BA}\left[\frac{M_0(B)}{M_0(A)}\right] \tag{24}$$

should be obtained. Provided that this relation is satisfied within experimental error, one may assume that departures from the two-site exchange scheme, caused by, for example, the existence of enzymatic intermediates, competing reactions, or reactions involving NMR-invisible substrate pools, are negligible. In that case, the values obtained for $k_{AB}$ and $k_{BA}$ define the true kinetics of the reaction. Verifying the internal consistency of the data according to Eq. 24 is a crucial step in reaching this conclusion. Suppose, on the other hand, that

$$k_{AB} \neq k_{BA}\left[\frac{M_0(B)}{M_0(A)}\right]. \tag{25}$$

This result would imply that the two-site exchange network does not adequately account for the main features of the reaction. A modification of Eq. 1 must then be introduced and verified experimentally.

This is precisely the situation reported with respect to the creatine kinase reaction (1–4): the forward flux is greater than the reverse flux. To account for this apparent discrepancy, one could modify the simple two-site model describing the phosphorus-exchange system in the heart, diagrammed in the Introduction, in a number of ways. These include considering the presence of NMR-invisible metabolites (14), nonexchanging pools (4), additional reaction sites (2, 10), or a combination of these. In this study, we have chosen to apply the most straightforward modification of the two-site system, that is, explicit inclusion of a third site for phosphorus exchange, $P_i$. This was also the choice made by Ugurbil and colleagues (9, 10). Our conclusion that the discrepancy between the forward and reverse fluxes through the creatine kinase reaction can be resolved by correctly accounting for the presence of ATPase reactions supports the conclusions drawn by Ugurbil and colleagues (9, 10) using a similar approach. They also support the speculations made by Matthews et al. (2) that the presence of competing ATPase reactions account for the apparent discrepancy between forward and reverse flux. Based on calculations showing that the velocity of the creatine kinase reaction exceeds the rate of ATP synthesis by a factor of 8 to 16, Bittl and Ingwall (4) concluded that the presence of other ATP-utilizing reactions may not be a major factor accounting for the apparent discrepancy. Results reported here show that, although the ratio of the rates of ATP synthesis via the creatine kinase reaction and via all other NMR-observable ATP synthesis reactions is indeed high (Table I), the three-site exchange network, including ATPase reactions, more accurately defines high-energy phosphate exchange in the beating heart. Although the three-site exchange network provides the expected value of 1 for the ratio of ATP synthesis flux to ATP degradation flux, the errors in the flux values are large. Thus we cannot exclude the possibility that the existence of metabolite compartments could contribute to the discrepancy. Our results do suggest, however, that such a contribution should be small.

The double saturation method used by Ugurbil and colleagues (9, 10) and the one reported here differ. Each has advantages. The chief advantage of the technique described by Ugurbil (9) is that it allows for the formal elimination of the competing reaction from the Bloch equations describing the reaction system. On the other hand, the transient magnetization transfer experiment that we employ has the advantage that kinetic constants and spin-lattice relaxation constants are derived from the same data set. Although our technique allows only for the direct measurement of the sum of $k_r$ and $k'_r$ for the creatine kinase-ATPase system, while the technique described by Ugurbil (9) provides $k_r$ by itself, obtaining the sum ($k_r + k'_r$) suffices to confirm flux balance and the adequacy of the three-site model (Eq. 17) for this system. This in turn

validates a derivation of $k_r$ and $k_r'$ from $k_f$ and $k_f'$, which are provided by standard single-saturation techniques, by using detailed balance:

$$k_r = k_f\left(\frac{[CP]}{[[\gamma\text{-P}]ATP]}\right), k_r' = k_f'\left(\frac{[P_i]}{[[\gamma\text{-P}]ATP]}\right), \quad (26)$$

Alternatively, $k_r$ may be obtained through a separate experiment, if desired, by applying a long-time saturation at $P_i$, so that the CP and [$\gamma$-P]ATP resonances reach a steady state, denoted respectively by $M_{ss}(CP)$ and $M_{ss}([\gamma\text{-P}]ATP)$. Eq. 18 becomes

$$0 = \frac{M_0(CP) - M_{ss}(CP)}{T_1(CP)} - k_f M_{ss}(CP) + k_r M_{ss}([\gamma\text{-P}]ATP), \quad (27)$$

which may be solved explicitly for $k_r$, since $T_1(CP)$ and $k_f$ have already been determined. Similarly, a long-time saturation at CP would allow $k_r'$ to be obtained directly.

An additional application of the transient magnetization transfer experiment reported here is the ability to detect multiple metabolite pools defined by different $T_1$'s. Since intracellular ATP exists in a cytosolic pool in fast exchange with CP and $P_i$, and in a mitochondrial pool which may have a different ATP $\rightleftharpoons$ $P_i$ exchange rate, this feature would have applications to the problem of defining more fully high-energy phosphate exchange in biological samples. To illustrate, consider a modification of Eq. 1 in which A is composed of two pools, one, $A^e$, exchanging with B, and another, $A^n$, not exchanging:

$$\begin{array}{c} A^e \underset{k_{AeB}}{\overset{k_{BAe}}{\rightleftharpoons}} B \\ + \\ A^n \end{array} \quad (28)$$

The solution of the appropriate Bloch equations for an inversion–recovery experiment performed with saturation at B (which may in general represent more than one species, e.g., $P_i$ and CP in the present application) is

$$M(A)(t) = M(A^e)(t) + M(A^n)(t) = M_0(A^e)\left\{\frac{\tau(A^e)}{T_1(A^e)} - \left[\frac{\tau(A^e)}{T_1(A^e)} + 1\right]\exp\left[\frac{-t}{\tau(A^e)}\right]\right\} + M_0(A^n)\left\{1 - 2\exp\left[\frac{-t}{T_1(A^n)}\right]\right\}. \quad (29)$$

This shows explicitly that, in general, measuring this recovery from inversion yields a value for $\tau(A^e)$ only in the case that the chemical–kinetic lifetimes of A in the two compartments, $\tau(A^e)$ and $T_1(A^n)$, are very different, so that the two exponentials in Eq. 29 can be resolved. However, the solution to the Bloch equations for a transient saturation–transfer experiment performed on this system is

$$M(A)(t) = M(A^e)(t) + M(A^n)(t) = M_0(A^e)\left\{\tau(A^e)k_{AeB}\exp\left[\frac{-t}{\tau(A^e)}\right] + \left[\frac{\tau(A^e)}{T_1(A^e)}\right]\right\} + M_0(A^n). \quad (30)$$

Saturation transfer data fitted to Eq. 30 will yield a value for $\tau(A^e)$. $T_1(A^n)$ can then be determined from an inversion–recovery experiment as defined by Eq. 29, since the exponential time constant involving $\tau(A^e)$ appearing in that equation is known. This permits the determination of the coefficients of the exponential terms and constant term in Eq. 29, which may be used further to calculate $M_0(A^e)$, $M_0(A^n)$, $k_{AeB}$, and $T_1(A^e)$. Thus, in principle, two pools defined by different $T_1$'s may be detected and characterized by combining the results of a transient saturation–transfer experiment with the results of an inversion–recovery experiment.

To summarize, we have extended the NMR technique of transient saturation transfer in order to properly account for the kinetics of phosphate exchange in the perfused rat heart. Previous work, allowing for only two sites of exchange for phosphorus (1–4), has resulted in an apparent violation of detailed balance in this system. Our treatment, appropriate for a three-site exchange network, provides one method of resolving this paradox and permits a direct demonstration of ATP homeostasis in vivo.

This research was supported by National Institutes of Health grant HL26215.

R. G. S. Spencer was supported by a Whitaker Foundation Fellowship.

*Received for publication 18 January 1988 and in final form 8 June 1988.*

## REFERENCES

1. Nunnally, R. L., and D. P. Hollis. 1979. Adenosine triphosphate compartmentation in living hearts: a phosphorus nuclear magnetic resonance saturation transfer study. *Biochemistry.* 18:3642–3646.
2. Matthews, P. M., J. L. Bland, D. G. Gadian, and G. K. Radda. 1982. A $^{31}$P-NMR saturation transfer study of the regulation of creatine kinase in the rat heart. *Biochim. Biophys. Acta.* 721:312–320.
3. Kobayashi, K., E. T. Fossel and J. S. Ingwall. 1982. Control of the creatine kinase reaction in the isolated perfused rat heart. *Fed. Proc.* 41:1740.
4. Bittl, J. A., and J. S. Ingwall. 1985. Reaction rates of creatine kinase and ATP synthesis in the isolated rat heart. *J. Biol. Chem.* 260:3512–3517.
5. Forsen, S., and R. A. Hoffman. 1964. Exchange rates by nuclear magnetic multiple resonance. III. Exchange reactions in systems with several nonequivalent sites. *J. Chem. Phys.* 40:1189–1196.
6. Forsen, S., and R. A. Hoffman. 1963. A new method for the study of moderately rapid chemical exchange rates employing nuclear magnetic double resonance. *Acta Chem. Scand.* 17:1787–1788.
7. Forsen, S., and R. A. Hoffman. 1963. Study of moderately rapid chemical exchange reactions by means of nuclear magnetic double resonance. *J. Chem. Phys.* 39:2892–2901.

8. Perrin, C. L., and E. R. Johnston. 1979. Saturation-transfer studies of three-site exchange kinetics. *J. Magn. Reson.* 33:619–626.
9. Ugurbil, K. 1985. Magnetization-transfer measurements of individual rate constants in the presence of multiple reactions. *J. Magn. Reson.* 64:207–219.
10. Ugurbil, K., M. Petein, R. Maidan, S. Michurski, and A. H. L. From. 1986. Measurement of an individual rate constant in the presence of multiple exchanges: application to myocardial creatine kinase reaction. *Biochemistry.* 25:100–107.
11. Koretsky, A. P., and M. W. Weiner. 1984. $^{31}$Phosphorus nuclear magnetic resonance magnetization transfer measurements of exchange reactions in vivo. *In* Biomedical Magnetic Resonance. A. Margulis and T. James, editors. Radiology Research and Education Foundation, San Francisco. 209–230.
12. Ingwall, J. S. 1982. Phosphorus nuclear magnetic resonance spectroscopy of cardiac and skeletal muscles. *Am. J. Physiol.* 242:H729–H744.
13. Bevington, P. R. 1969. Data Reduction and Error Analysis for the Physical Sciences. McGraw-Hill Book Company, New York. 56–65.
14. Zahler, R., J. A. Bittl, and J. S. Ingwall. 1987. Analysis of compartmentation of ATP in skeletal and cardiac muscle using $^{31}$P nuclear magnetic resonance saturation transfer. *Biophys. J.* 51:883–892.